Volume 14, Number 3, 2021. pp. 255-265

Jordan Journal of Physics

ARTICLE

Effect of Sr - Transition Metal Substitution on Electronic and Mechanical Properties of Mg_2Si: A DFT Study

A. S. Olayinka[a], **O. E. Odeyemi**[b] and **T. C. Olayinka**[c]

[a] *Department of Physics, Edo State University, Uzairue, Edo State, Nigeria.*

[b] *Department of SLT, Federal College of Animal Health and Production Technology, Ibadan, Nigeria.*

[c] *Department of Mathematical & Physical Sciences, Samuel Adegboyega University, Ogwa, Nigeria.*

Doi: **https://doi.org/10.47011/14.3.8**

Received on: 02/07/2020; *Accepted on: 6/10/2020*

Abstract: Recently, magnesium alloys have attracted scientific interest due to their technological importance in thermoelectric, piezoelectric, photo-voltaic and infrared photonics applications. The electronic and elastic properties of MgXSi (X = Mg, Sr) compounds were investigated in this work, using the density functional theory (DFT) with pseudo-potential plane-waves (PPW) approach as implemented in Quantum Espresso code. The results of the elastic constants of Mg_2Si are in agreement with the previous theoretical results and favourably compared with experimental data. The electronic band structures of these semiconductors were calculated to give narrow indirect and direct band gaps of Mg_2Si and MgSrSi, respectively. Our results show that the two compounds are mechanically stable. The Pugh's ratio, B/G, indicated that Mg_2Si and MgSrSi are brittle and ductile in nature. The estimated anisotropy parameter, A, shows that Mg_2Si has a higher degree of elastic isotropy in comparison to MgSrSi. Three-dimensional (3D) projection of Young's modulus and area modulus of the compounds was presented.

Keywords: Electronic structure**,** Elastic constants, Mechanical properties, Mg_2Si, MgSrSi.

PACS: 31.15.A-, 62.20.F-, 71.55.-i, 71.20.Be.

Introduction

Magnesium has recently become an important engineering material due to its abundance in the earth, less toxicity and cost-effectiveness compared to other competing materials for various technological applications [1, 2]. This has led to continuous and significant studies of magnesium-based alloys and compounds in the recent years due to their potentials for use in several technological applications, such as; thermoelectric, piezoelectric, photo-voltaic and infrared photonics [2, 3, 4]. Magnesium also possesses many other attractive properties, such as high damping capacity, electromagnetic shielding, thermal conductivity, good machinability and high recycling potential [2]. Moreover, Mg-based alloys are of great interest due to its low density (~1.74 g/cm^3) and high specific strength and stiffness compared to many other engineering materials, like steel, aluminium and polymer-based composites [5]. Magnesium alloys have been known to be among the lightest structural materials and have applications in several areas, like aerospace manufacturing and automobile industry [6, 7]. All these aforementioned attributes and features are our motivation to study these alloys.

Corresponding Author: A. S. Olayinka **Email**: akinola.olayinka@edouniversity.edu.ng

Several studies have been carried out on the mechanical alloy of tin (Sn) into magnesium silicide (Mg_2Si) to display better-detailed properties and thermoelectric properties than Mg_2Si. Difficulties encountered during the experimental set up include variations in temperature of the constituent elements and contamination in material processing [8, 9]. Magnesium silicide is one of the prominent silicides in solid-state application due to its compatibility with silicon, which is a based material for solid-state devices and electronics. This material has high thermal stability as well as desirable oxidization resistance properties, which makes it fit as a green material for semiconductor applications. This material is also known as a semiconductor with a narrow band gap, which has been used at a wavelength range of 1.2 to 1.8 micrometers as an infrared detector [8-10]. Doping and alloying have been used to enhance properties of semiconductors for optimum applications in optoelectronics and energy generation [11-13]. Elastic properties of the Mg_2Si structure under pressure have been reported by Zhang et al. (2018). Their calculated elastic constants are stable at a minimal pressure range of 0 to 7 GPa under Born's stability conditions at low pressures [9]. Hao et al. (2009) reported the experimental measurement of the compressive-to-phase transformation characteristics of Mg_2Si at room temperature [14]. Some works of literature only report elastic constants and Young's modulus, leaving out other elastic properties in their work. In this work, we present first-principle calculations of structural, mechanical and elastic properties of MgXSi (X = Mg, Sr) in antifluorite face-centered cubic (FCC) structure. The elastic constants, bulk modulus B, Young's modulus E, shear modulus G, Poisson's ratio, Zener's anisotropy A and Pugh's ratio B/G of Mg_2Si and MgSrSi are computed and discussed. The results are compared with available experimental and theoretical results.

Computational Details

Our calculations were carried out using plane-wave density functional theory (DFT) [15] using the Projected Augmented Wave (PAW) PBE functional which defines the exchange-correction energy. A projected augmented wave (PAW) type of pseudopotentials was employed. The pseudo-potentials used in the modeling of these materials are Mg.pbe-spn-kjpaw_ps l.1.0.0.UPF, Si.pbe-n-kjpaw_ps l.1.0.0.UPF and Sr.pbe-spn-kjpaw_ps l.1.0.0.UPF. The calculation of the pseudopotential *i*nvolves *Mg:* $2p^6\ 3s^2$ *and Si:* $3s^2\ 3p^2$ *and Sr:* $4p^6 5s^2$ orbitals. Relaxation of the atomic structures was carried out using the Broyden-Fletcher-Goldfarb-Shanno method [16]. Brillouin zone is sampled using Monkhorst–Pack scheme [17] with a k-point grid of 8 x 8 x 8. The computations were carried out using thermo_pw [18] on the Quantum Espresso (QE) code [19-21]. The elasticity of the compounds was post-processed and analyzed (Self-consistent Elasticity of Multi-phase Aggregates (SC-EMA) code [22-24] and EIAM code [25].

Results and Discussion

Structural and Electronic Properties

The atomic structures of Mg_2Si and MgSrSi intermetallic compounds are known to crystallize in FCC lattice and the space group 225 $Fm\bar{3}m$ of antifluorite structural type. The atom of Si is located at the (0, 0, 0) sites in a primitive cell and two equivalent Mg atoms occupy the (a/4) (1, 1, 1) and (3a/4) (1, 1, 1) sites, where *a,* is the lattice constant [26]. The schematic diagrams of the crystal structures of these alloys are shown in Fig. 2 and their X-ray diffraction patterns are shown in Fig. 3. Interaction of X-rays (a spectrum of electromagnetic wave) with a crystalline substance results in a diffraction pattern which helps in the description of the crystal properties. X-ray diffraction is useful in crystal structure characterization, as well as obtaining useful crystal information, like lattice constants, crystallite size and degree of graphitization [27]. We calculated the electronic band structures of Mg_2Si and MgSrSi compounds at their equilibrium lattice constants, as shown in Figs. 4 and 5, respectively. For both compounds studied, the electronic band structure of Mg_2Si shows an indirect band gap of 0.39eV between Γ - X with the Maximum Valence Band (MVB) observed at gamma point, while the Conduction Band Minimum (CBM) is at the X point of the Brillouin zone (Fig. 4). The electronic band structure of MgSrSi depicts a direct band gap of 0.91eV with respect to the Fermi level and its Maximum Valence Band (MVB) and the Minimum Conduction Band (MCB) occurred at point X of the Brillouin zone (Fig. 5). The two compounds theoretically display semiconducting behaviour due to their

narrow band gaps. The electronic band gap was increased with 0.52eV with the substitution of Sr for one atom of Mg from indirect band gap of Mg_2Si (0.39eV) to direct band gap of MgSrSi (0.91eV). The Brillouin zone representation for FCC Mg_2Si and MgSrSi is shown in Fig. 1.

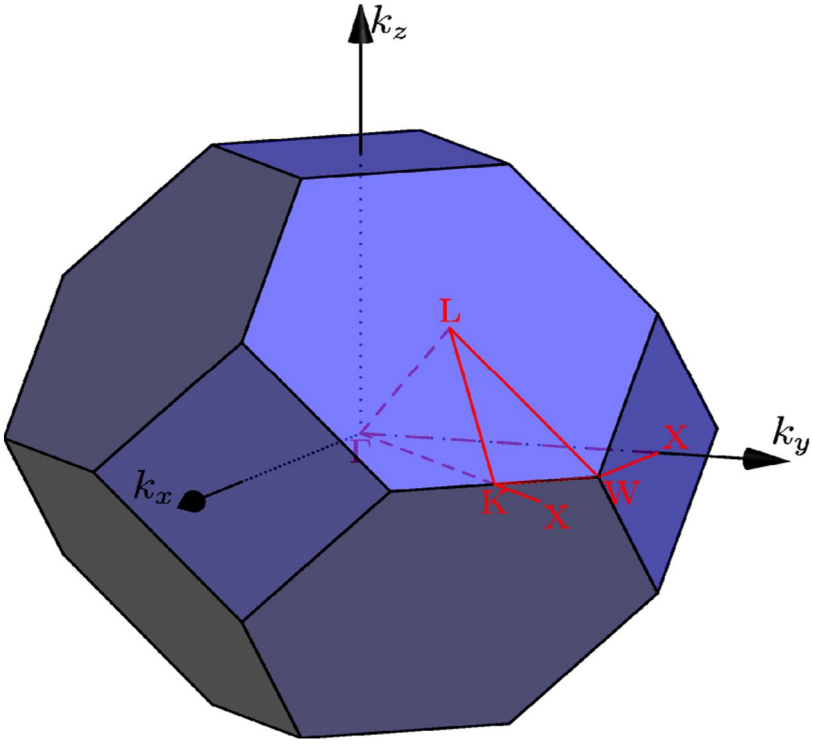

FIG. 1. Brillouin zone for FCC Mg_2Si and MgSrSi.

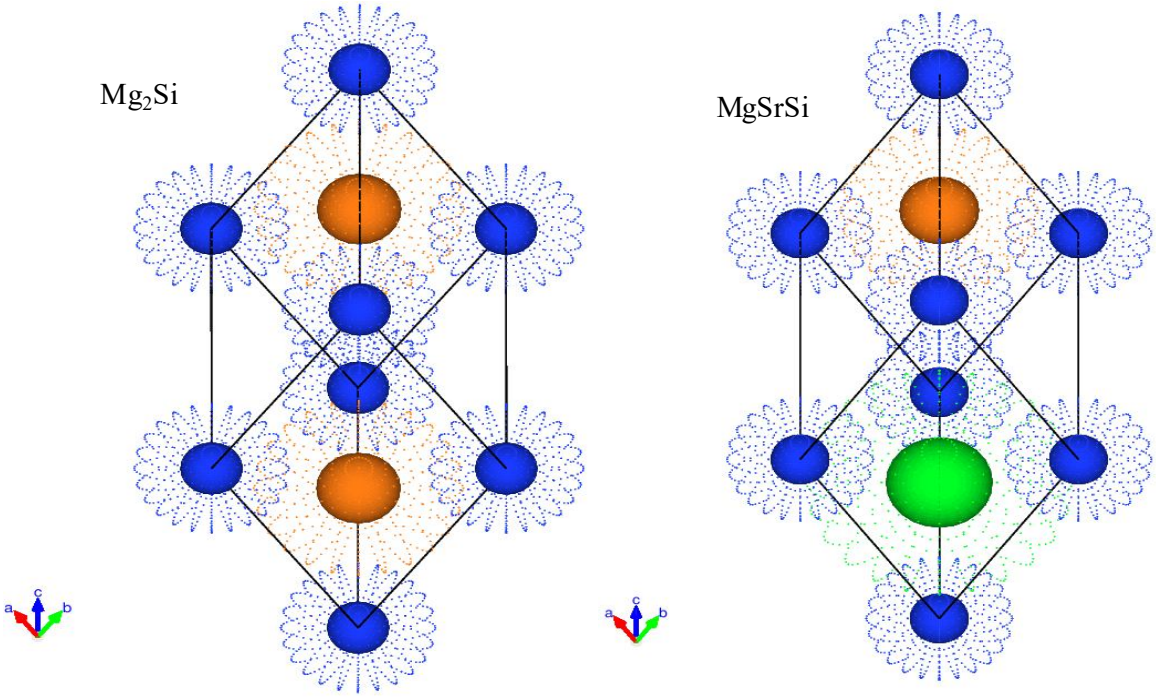

FIG. 2. Crystal structure of Mg_2Si and MgSrSi. Blue ball and gold ball represent Si and Mg, respectively, while green ball represents the substituted Sr atom for Mg.

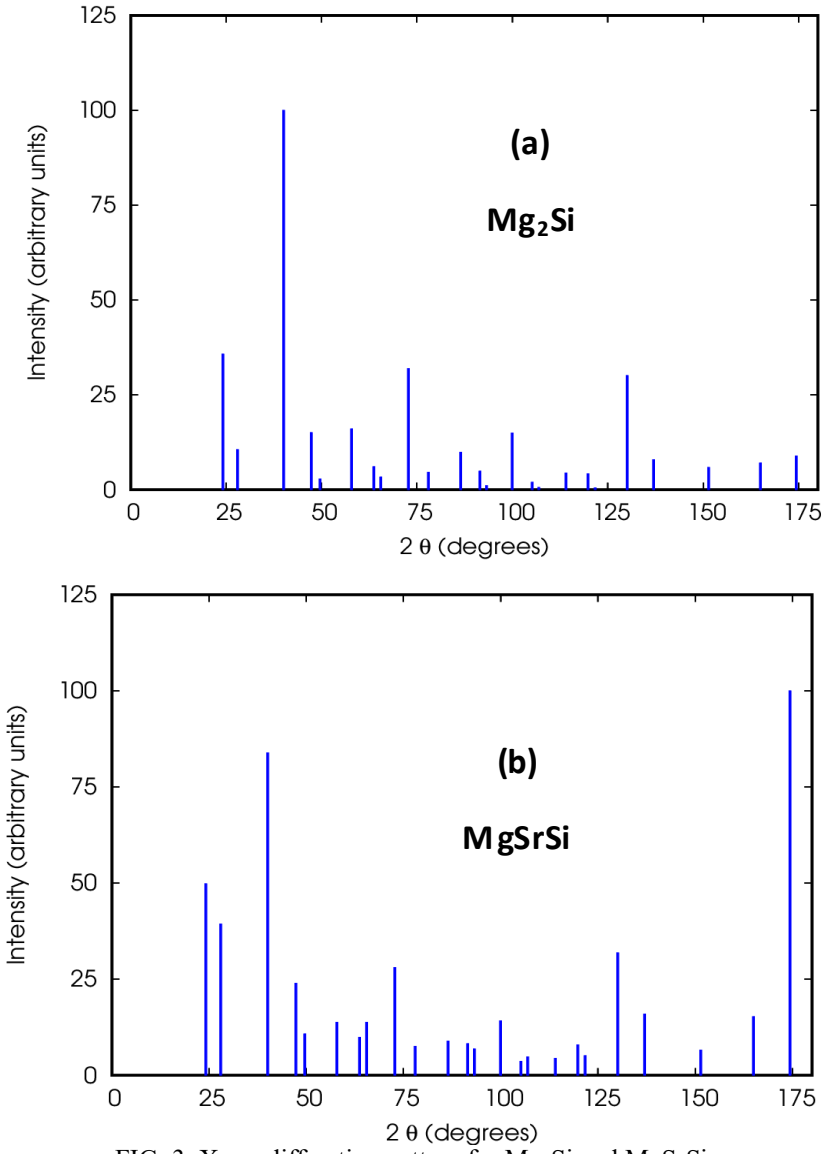

FIG. 3. X-ray diffraction pattern for Mg_2Si and MgSrSi.

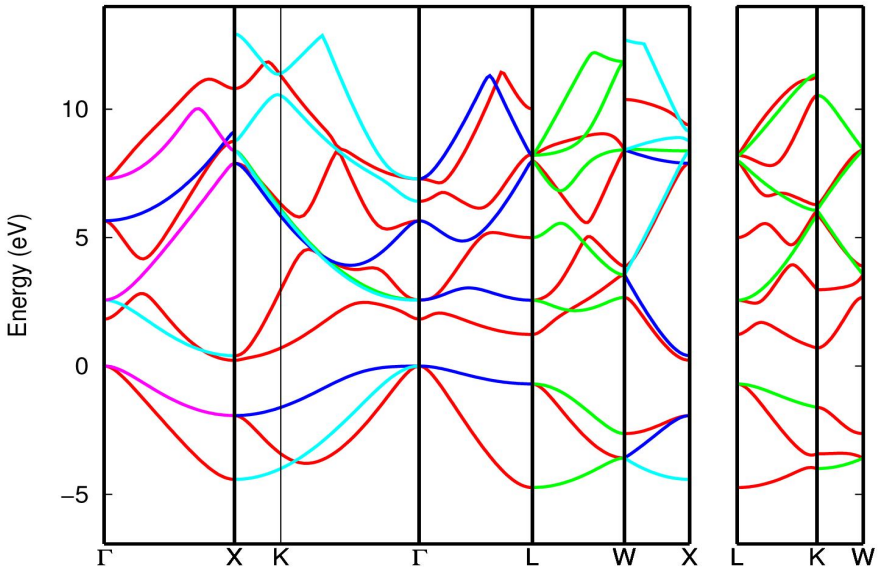

FIG. 4. Electronic band structure for Mg_2Si with an indirect band gap of 0.39eV between Γ and X.

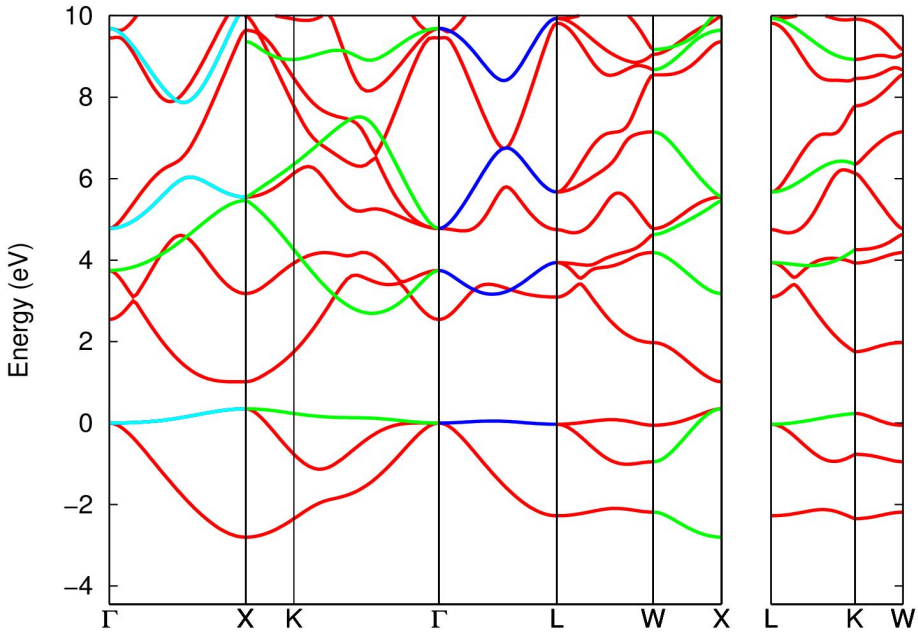

FIG. 5. Electronic band structure for MgSrSi with a direct band gap of 0.91eV at X point.

Elastic and Mechanical Properties

The elastic and mechanical properties of MgXSi (X = Mg, Sr) compounds were calculated and are shown in Table 1. Elastic constants (*Cij*) of any material play an important role in understanding its mechanical properties. C_{ij} are the elastic constants of the crystal and its structure has been fully relaxed under a given set of exchange-correlation potential functions and obtained an equilibrium structure with a minimum total energy. Before a material can be termed a mechanically stable material, the Born's stability conditions of cubic crystal [28] must be satisfied which are: $C_{11} > 0$, $C_{11} - C_{12} > 0$, $C_{44} > 0$, $C_{11} + 2C_{12} > 0$ and $C_{12} < B < C_{11}$. The results of C_{11}, C_{12} and C_{44} obtained as presented in Table 1 clearly show that the studied MgXSi (X=Mg, Sr) compounds are mechanically stable having satisfied the aforementioned conditions. The lattice constant, a = 6.341 *Å* and elastic parameters, C_{ij} (*GPa*) of Mg_2Si (C_{11} = 116.0 *GPa*, C_{12} = 22.6 *GPa* and C_{44} = 45.2 *GPa*) are in good comparison with the available theoretical [2, 25] and experimental data [29].

As it is well known, elastic properties such as bulk modulus (B) determine the resistance of any material fracture and the shear modulus (G) gives the resistance to plastic deformation. The B/G ratio, which is also described as Pugh's ratio, is used to understand the ductile/brittle behaviour of solids [30]. The critical value is 1.75, where greater than that value, the material is regarded as ductile [30, 31]. In this work, the B/G ratios of the two compounds were found to be 1.18 and 5.89 for Mg_2Si and MgSrSi, respectively. This shows that Mg_2Si alloy indicates brittle behavior, while MgSrSi is ductile in nature, based on their B/G ratios values.

The elastic anisotropy of crystals is an important factor in material science. There are different ways by which elastic anisotropy can be estimated theoretically. The Zener's anisotropy parameter $A = 2C_{44} / (C_{11} - C_{12})$ is usually adopted for this purpose [32, 33] . The degree of deviation of Zener's anisotropy parameter from unity (1) means the degree of elastic anisotropy. Mg_2Si is elastically isotropic with A = 0.96 and a little degree of elastic anisotropy is observed in MgSrSi with A = 0.42, as presented in Tables 1 and 2.

To calculate the polycrystalline modulus, two approximation methods are employed which are the Voight method and the Reuss method. Using energy considerations, Hill showed that the Voight and Reuss equations stand for upper and lower limits of realistic polycrystalline constants and recommended that a practical estimate of the bulk and shear moduli should be the arithmetic means of the extremes. Elastic properties (such as bulk modulus, shear modulus, Young's modulus and Poisson's ratio) are calculated through Equations (1) – (6) in the Voight-Reuss-Hill approximation and their values are presented in Table 2.

TABLE 1. Calculated elastic properties: The lattice constant *a* (Å), the elastic constants C_{11}, C_{12} and C_{44} (GPa), Young's moduli (*E*, in GPa), shear moduli (*G*, in GPa), Poisson's ratios (*v*), Zener's anisotropy A and the B/G ratio of MgXSi (X=Mg, Sr) compounds compared with other results.

Material	a (Å)	C_{11}	C_{12}	C_{44}	*E*	*G*	*V*	*A*	*B/G*
Mg_2Si	6.341*	116.0*	22.6*	45.0*	106.7*	45.6*	0.17*	0.96*	1.18*
	6.295[a]	121.2[a]	23.7[a]	49.5[a]	113.5[a]	49.2[a]	0.161[a]	-	1.14[a]
	6.35[b]	118.82[b]	22.27[b]	44.96[b]	111.79[b]	46.25[b]	0.15[b]	-	1.18[b]
	6.338[c]	126.0[c]	26.0[c]	48.5[c]	-	-	-	-	-
MgSrSi	6.361*	166.8*	67.2*	20.9*	48.07*	17.02*	0.42*	0.42*	5.89*

* = This Work a = [36] b = [2] c = [37]

TABLE 2. Calculated mechanical parameters' values of Mg_2Si and MgSrSi using Voight, Ruess and Hill approximations.

	Mg_2Si	**MgSrSi**
A	0.96	0.42
1-A	0.4	0.58
A_G	1.039	2.377
$B_V = B_R = B_H$ (GPa)	53.71	100.3
$\beta_V = \beta_R = \beta_H$ (10^{-3} /GPa)	6.2059	3.3211
G_V (GPa)	45.63	32.493
G_R (GPa)	45.62	27.27
G_H (GPa)	45.63	29.88
E_V (GPa)	106.69	87.985
E_R (GPa)	106.66	75.016
E_H (GPa)	106.67	81.552
ν_V	0.168	0.3539
ν_R	0.169	0.375
ν_H	0.169	0.365
B_V / G_V	1.18	3.087
B_R / G_R	1.18	3.678
B_R / G_R	1.18	3.357

A, anisotropy factor; A_G, anisotropy in shear moduli; B, bulk moduli; β, compressibility; G, shear moduli; E, Young's modulus; v, Poisson's ratio.

$$B = \frac{C_{11} + 2C_{12}}{3} \quad (1)$$

$$G_v = \frac{C_{11} - C_{12} + 3C_{44}}{5} \quad (2)$$

$$G_R = \frac{5(C_{11} - C_{12})C_{44}}{4C_{44} + 3(C_{11} - C_{12})} \quad (3)$$

$$G = \frac{G_v + G_R}{2} \quad (4)$$

where *B*, *G* and C_{ij} (C_{11}, C_{12} and C_{44}) are the bulk moduli, shear moduli and elastic parameters; G_V and G_R are Voigt's and Reuss's shear moduli, respectively. Hence, the Young's modulus *E* and the Zener's anisotropy factor *A* are computed as follows [34]:

$$E = \frac{9GB}{3B + G} \quad (5)$$

$$A = \frac{2C_{44} + 2C_{12}}{C_{11} - C_{12}} \quad (6)$$

Young's modulus, which is the ratio of strain to stress, is used to determine the stiffness of a material. On the other hand, area modulus is the ratio of an equibiaxial stress to the relative area change in the planes in which the stress acts. It is an intermediate elastic property between Young's modulus and bulk modulus, which is computed in isotropic elasticity [35]. The results computed in Table 2 show that Mg_2Si with E_H = (106.66 GPa) is stiffer than MgSrSi (E_H = 75.016 *GPa*). SC-EMA (Self-consistent Elasticity of Multi-phase Aggregates [22-24] and EIAM code [25] were used as post-processor for elasticity of Mg_2Si and MgSrSi to plot the three-dimensional (3D) image of area modulus and Young's modulus, as shown in Figs. 6 – 10. These Young's moduli are more intuitive than the bulk modulus to indicate the anisotropy of the crystals. These three-dimensional projections of Young's moduli indicate the directional dependences of the Young's moduli of the Mg_2Si and MgSrSi crystals. This result is consistent with the anisotropy factor given in

Table 1 with Mg_2Si is isotropic and MgSrSi crystal deviates a bit from isotropic behavior. Figs. 6 and 7 were generated using 200 data points each. Fig. 6 shows the 3D projection of Young's modulus and area modulus for Mg_2Si. The computed homogenized polycrystalline Young's modulus is 102.01 GPa, while the cubic single crystals 001, 110 and 111 planes' area moduli of elasticity were 59.89 GPa, 61.42 GPa and 61.85 GPa, respectively. Fig. 7 shows the 3D projection of Young's modulus and area modulus for MgSrSi. The computed homogenized polycrystalline Young's modulus is 82.81 GPa, while the cubic single crystals 001, 110 and 111 planes' area moduli of elasticity were 91.73 GPa, 53.17 GPa and 47.91 GPa, respectively. Fig. 8 shows the 3D and 2D projections of Poisson's ratio as computed for Mg_2Si and MgSrSi, respectively. Minimum and maximum dimensionless Poisson's ratios of 0.2 and 0.47 were measured for Mg_2Si with corresponding transverse maximum and minimum of (0.71 -0.70 0.00) and (0.00 0.00 -1.00), respectively along x y z. For MgSrSi, minimum and maximum dimensionless Poisson's ratios of 0.11 and 0.15 were recorded with corresponding transverse maximum and minimum of (0.71 -0.70 0.00) and (0.00 0.00 -1.00), respectively along x y z. Fig. 9 shows the 3- and 2- dimensional projections of shear modulus for Mg_2Si and MgSrSi, respectively. Shear modulus is one of the important quantities, as it determines the stiffness of a material. Computed shear moduli for Mg_2Si and MgSrSi were 45.63 GPa and 32.493 GPa, respectively, which compared well with our calculated homogenized polycrystalline shear moduli of 43.81 GPa and 30.53 GPa for Mg_2Si and MgSrSi, respectively using SC-EMA code [22-24]. Fig. 10 shows the 3D and 2D projections of sound velocities for Mg_2Si and MgSrSi, respectively. Minimum and maximum acoustic modes were 22.60 and 35.50 for Mg_2Si and 67.20 and 72.95 for MgSrSi, respectively. The acoustic modes for Mg_2Si and MgSrSi suggest that MgSrSi has a higher potential for acoustic application.

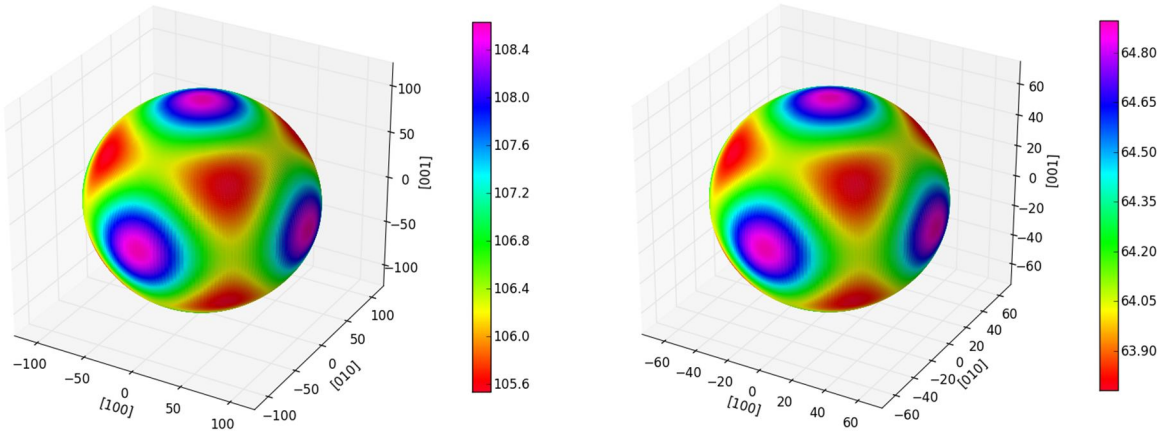

(a) (b)

FIG. 6. 3D projection for (a) Young's modulus and (b) area modulus of Mg_2Si.

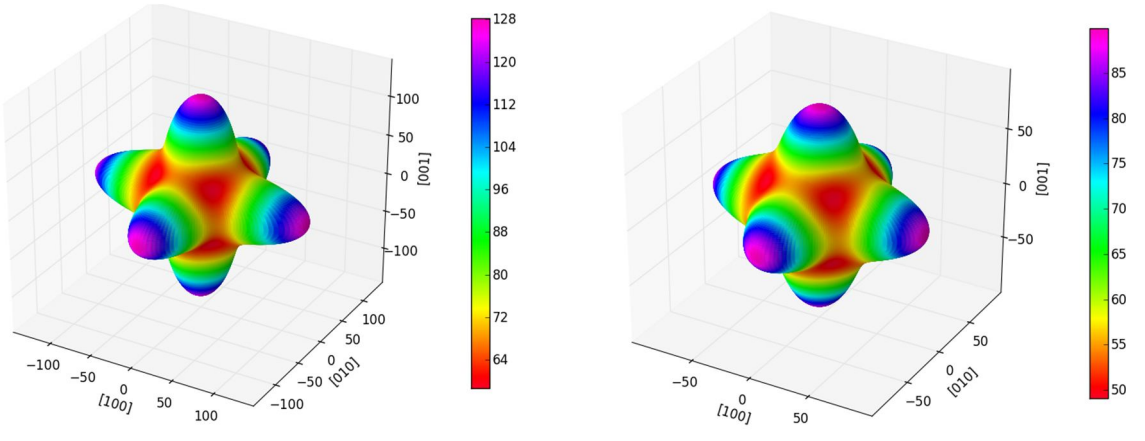

(a) (b)

FIG. 7. 3D projection for (a) Young's modulus and (b) area modulus of MgSrSi.

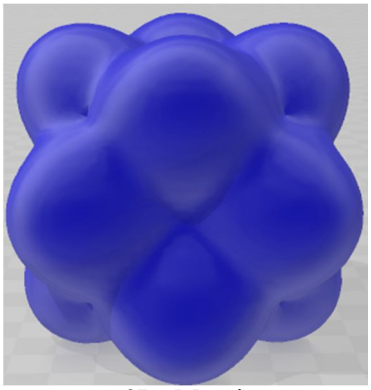

3D--Mg_2Si

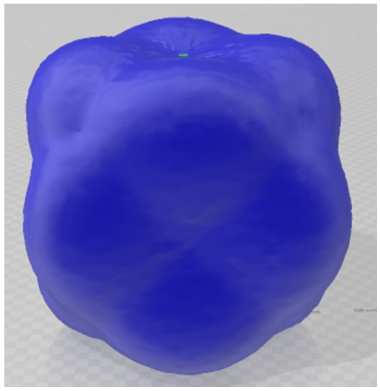

3D--MgSrSi

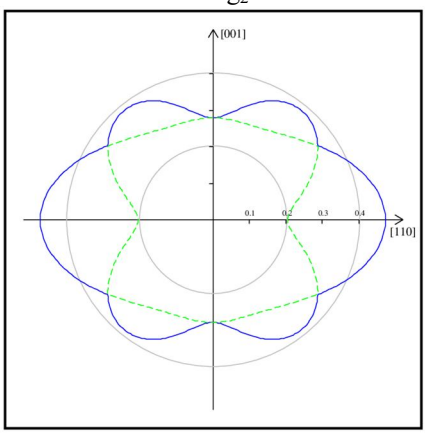

2D--Mg_2Si

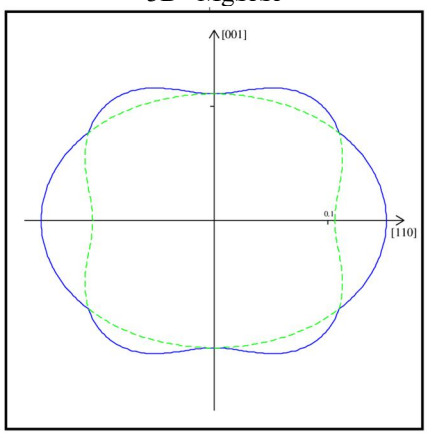

2D--MgSrSi

FIG. 8. 3D and 2D projections of Poisson's ratio for Mg_2Si and MgSrSi, respectively.

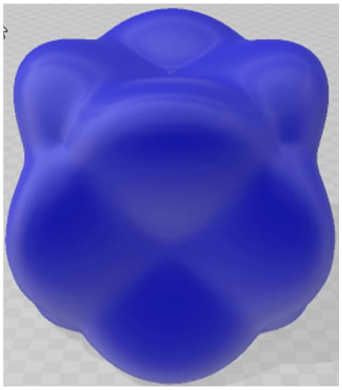

3D--Mg_2Si

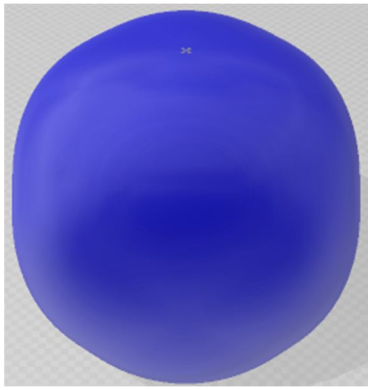

3D--MgSrSi

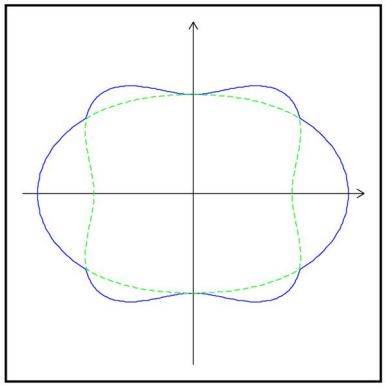

2D--Mg_2Si

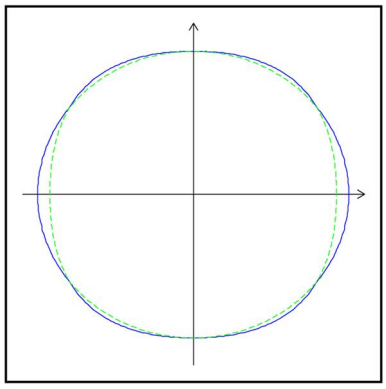

2D--MgSrSi

FIG. 9. 3D and 2D projections of shear modulus for Mg_2Si and MgSrSi, respectively.

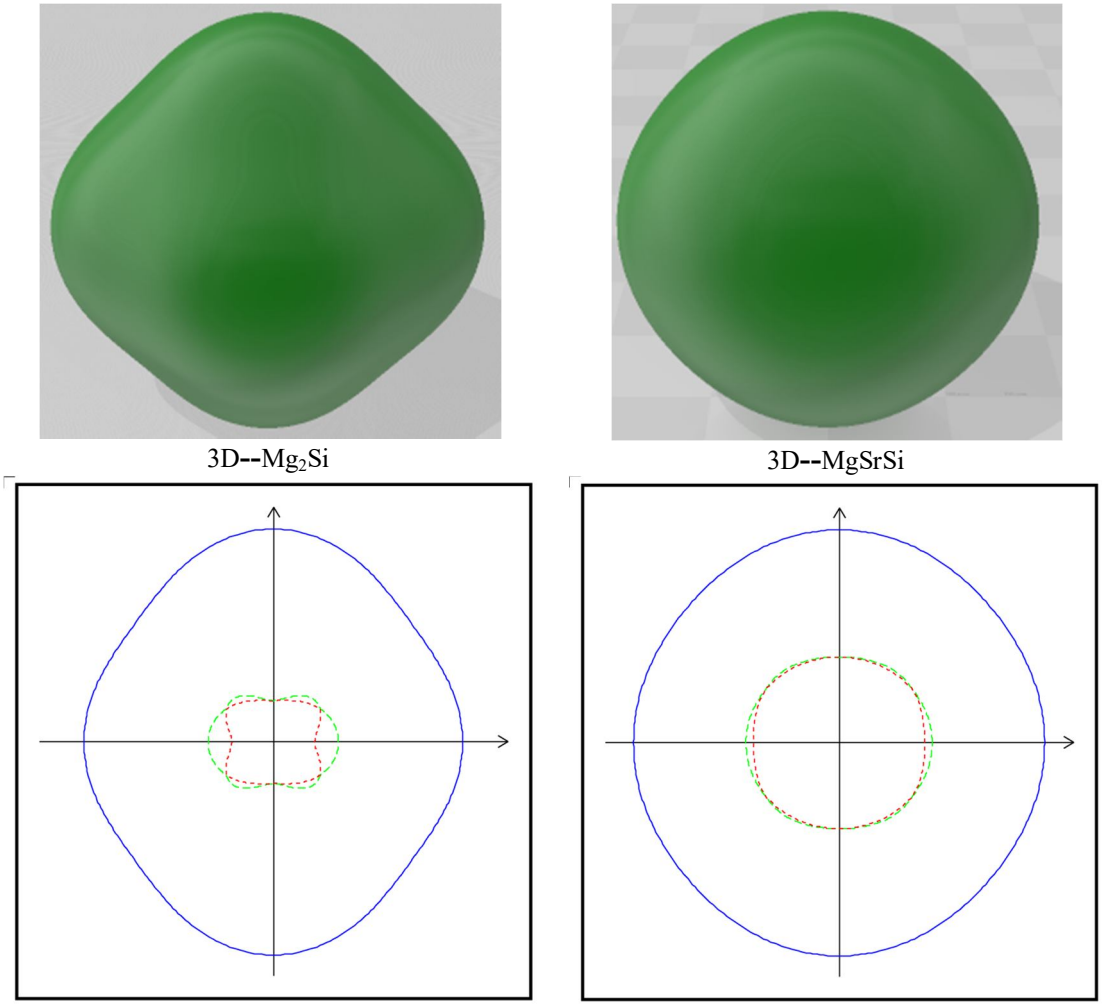

FIG. 10. 3D and 2D projections of sound velocities for Mg_2Si and MgSrSi, respectively.

Conclusion

In the present theoretical study, the structural, elastic and mechanical properties of Mg_2Si and MgSrSi intermetallic compounds have been investigated employing the DFT with pseudo-potential plane-waves (PPW) approach using Projector Augmented Wave (PAW) method for the exchange and correlation potential. The results obtained for the optimized lattice parameter (a) agree with the available theoretical and experimental data. The elastic constants C_{ij} and related polycrystalline mechanical parameters, such as bulk modulus B, Young's modulus E, shear modulus G and Poisson's ratio, were computed. Zener's anisotropy parameter, A, and the B/G ratio were also estimated. From the results, it is concluded that the elastic constants of Mg_2Si are quite in good agreement with theoretical results already recorded on the subject and compare favourably with experimental data. The two compounds studied are mechanically stable having satisfied the elastic stability criteria. The three-dimensional Young's modulus of Mg_2Si also confirmed the computed results obtained by Zener's anisotropy factor A, which are nearly spherical, indicating that the crystal was isotropic. The studied compounds were classified as semiconducting materials having indirect band gap (0.39eV) and direct band gap (0.91eV) for Mg_2Si and MgSrSi, respectively in their electronic band structures.

References

[1] Liu, Y., Hu, W.C., Li, D.J., Zeng, X.Q. and Xu, C.S., Physica Scripta, 88(4) (2013) 045302.

[2] Na-Na, L., Ren-Bo, S. and Da-Wei, D., Chinese Physics B., 18 (5) (2009) 1979.

[3] Noda, Y., Kon, H., Furukawa, Y., Otsuka, N., Nishida, I.A. and Masumoto, K., Materials Transactions, JIM, 33 (9) (1992) 845.

[4] Schilz, J., Riffel, M., Pixius, K. and Meyer, H.J., Powder Technology, 105 (1-3) (1999) 149.

[5] Boucetta, S., Journal of Magnesium and Alloys, 2 (1) (2014) 59.

[6] Dieringa, H. and Kainer, K.U., "Magnesium and magnesium alloys", In: "Springer Handbook of Materials Data", 2nd Edn., (Springer, 2018).

[7] Kainer, K.U., "Magnesium: Alloys and Technology", (Wiley-VCH Verlag GmbH & Co. KGaA, 2003).

[8] Li, S., Li, X., Dong, C. and Jiang, X., Acta Physica Sinica, 59 (6) (2010) 4267.

[9] Zhang, J., Ma, H., Zhao, B., Wei, Q. and Yang, Y., AIP Conference Proceedings, 1971 (2018) 020018.

[10] Saravanan, R. and Robert, M.C., Journal of Alloys and Compounds, 479 (1-2) (2009) 26.

[11] Olayinka, A.S., Adetunji, B.I., Idiodi, J.O.A. and Aghemelon, U., International Journal of Modern Physics B, 33 (06) (2019) 1950036.

[12] Olayinka, A.S., Idiodi, O.A.J. and Nwankwo, W., In: Covenant Journal of Physical & Life Sciences (CJPL), 7 (2) (2019) 2354.

[13] Olayinka, A.S. and Bamidele, O., Journal of Mat., 25625 (6) (2016) 235.

[14] Hao, J., Zou, B., Zhu, P., Gao, C., Li, Y., Liu, D., Wang, K., Lei, W., Cui, Q. and Zou, G., Solid State Communications, 149 (17-18) (2009) 689.

[15] Kohn, W., Becke, A.D. and Parr, R.G., Journal of Physical Chemistry, 100 (31) (1996) 12974.

[16] Fletcher, R., "Practical Methods of Optimization", (Wiley Online Library, 2000).

[17] Monkhorst, H.J. and Pack, J.D., Physical Review B, 13 (12) (1976) 5188.

[18] Dal Corso, A., Journal of Physics: Condensed Matter, 28 (2016) 075401.

[19] Giannozzi, P., Baroni, S., Bonini, N., Calandra, M., Car, R., Cavazzoni, C., Ceresoli, D., … and Wentzcovitch, R., Journal of Physics: Condensed Matter, 21 (2009) 395502.

[20] Giannozzi, P., Andreussi, O., Brumme, T., Bunau, O., Buongiorno Nardelli, M., Calandra, M., Car, R., … and Baroni, S., Journal of Physics: Condensed Matter, 29 (2017) 465901.

[21] Giannozzi, P. and Cavazzoni, C., Nuovo Cimento Della Societa Italiana Di Fisica C., 32 (2) (2009) 49.

[22] Friák, M., Counts, W.A., Ma, D., Sander, B., Holec, D., Raabe, D. and Neugebauer, J., Materials, 5 (10) (2012) 1853.

[23] Titrian, H., Aydin, U., Friák, M., Ma, D., Raabe, D. and Neugebauer, J., Materials Research Society Symposium Proceedings, 1524 (2013) Mrsf12-1524-rr06-03.

[24] Zhu, L.F., Friák, M., Lymperakis, L., Titrian, H., Aydin, U., Janus, A.M., Fabritius, H.O., Ziegler, A., Nikolov, S., Hemzalová, P., Raabe, D. and Neugebauer, J., Journal of the Mechanical Behavior of Biomedical Materials, 20 (2013) 296.

[25] Marmier, A., Lethbridge, Z.A.D., Walton, R.I., Smith, C.W., Parker, S.C. and Evans, K.E., Computer Physics Communications, 181 (12) (2010) 2102.

[26] Folland, N.O., Physical Review, 158 (1967) 764.

[27] Iwashita, N., Materials Science and Engineering of Carbon, 2016 (2016) 7.

[28] Born, M., Huang, K. and Lax, M., American Journal of Physics, 23 (1955) 474.

[29] Schmidt, R.D., Case, E.D., Giles, J., Ni, J.E. and Hogan, T.P., Journal of Electronic Materials, 41 (2012) 1210.

[30] Pugh, S.F., The London, Edinburgh and Dublin Philosophical Magazine and Journal of Science, 45 (367) (1954) 823.

[31] Bannikov, V.V., Shein, I.R. and Ivanovskii, A.L., Physica Status Solidi - Rapid Research Letters, 1 (3) (2007) 89.

[32] Gschneidner, K., Russell, A., Pecharsky, A., Morris, J., Zhang, Z., Lograsso, T., Hsu, D., Lo, C.H.C., Ye, Y., Slager, A. and Kesse, D., Nature Materials, 2 (2003) 587.

[33] Yang, Y., Lu, H., Yu, C. and Chen, J.M., Journal of Alloys and Compounds, 485 (1-2) (2009) 542.

[34] Zener, C.M. and Siegel, S., Journal of Physical and Colloid Chemistry, 53 (9) (1949) 1468.

[35] Scott, N.H., Journal of Elasticity, 58 (3) (2000) 269.

[36] Tani, J.I. and Kido, H., Computational Materials Science, 42 (3) (2008) 531.

[37] Madelung, O., "Landolt-Börnstein: Numerical Data and Functional Relationships in Science and Technology - New Series", (Group III, Vol. 17e, Springer-Verlag, Berlin, 1983).